

Dalton Transactions

Accepted Manuscript



This is an *Accepted Manuscript*, which has been through the Royal Society of Chemistry peer review process and has been accepted for publication.

Accepted Manuscripts are published online shortly after acceptance, before technical editing, formatting and proof reading. Using this free service, authors can make their results available to the community, in citable form, before we publish the edited article. We will replace this *Accepted Manuscript* with the edited and formatted *Advance Article* as soon as it is available.

You can find more information about *Accepted Manuscripts* in the [Information for Authors](#).

Please note that technical editing may introduce minor changes to the text and/or graphics, which may alter content. The journal's standard [Terms & Conditions](#) and the [Ethical guidelines](#) still apply. In no event shall the Royal Society of Chemistry be held responsible for any errors or omissions in this *Accepted Manuscript* or any consequences arising from the use of any information it contains.

Cite this: DOI: 10.1039/c0xx00000x

www.rsc.org/xxxxxx

ARTICLE TYPE

Versatile Redox Reactivity of triaryl-*meso*-substituted Ni(II) Porphyrin†

Abdou K. D. Dimé, Charles H. Devillers,* H el ene Cattey and Dominique Lucas*

Received (in XXX, XXX) Xth XXXXXXXXXX 20XX, Accepted Xth XXXXXXXXXX 20XX

DOI: 10.1039/b000000x

5 The electrochemical oxidation of nickel(II) 5,15-*p*-ditolyl-10-phenylporphyrin (**1-Ni**) leads to the formation of different coupling products, with the distribution depending on the solvent nature (CH₂Cl₂/CH₃CN, CH₂Cl₂, DMF), the cell configuration (2 or 3 compartments) and the number of electron abstracted. In a two cell configuration (anode and cathode in the same compartment) in a CH₂Cl₂/CH₃CN mixture, nickel(II) 5-chloro-10,20-*p*-ditolyl-15-phenyl porphyrin (**1-Ni-Cl**) was isolated
10 in good yield. The mechanism of its formation is proposed. Switching to the three cell configuration, the *meso-β/meso-β* doubly fused dimer (**3-Ni**) is detected as the major product whereas in pure CH₂Cl₂, the singly bonded *meso-β* dimer (**2-Ni**) is the major product; in both cases a significant amount of **1-Ni-Cl** is also produced. These results are in accordance with the cyclic voltammetry analysis of **1-Ni** measured in CH₂Cl₂/CH₃CN and CH₂Cl₂ from which the voltammetric trace of **3-Ni** is, respectively, appearing or not.
15 Besides, in DMF the hydroxyporphyrin **1-Ni-OH** was detected as the major product. Moreover, *meso*-functionalization of **1-Ni** was performed by controlled potential electrolysis with triphenylphosphine as nucleophile leading to the phosphonium substituted derivative (**1-Ni-P⁺**) in good yield. Finally, unprecedented X-ray crystallographic structures of the **1-Ni**, **1-Ni-Cl**, **1-Ni-P⁺** and **3-Ni** are presented and their respective structural parameters are compared.

20 Introduction

Porphyrins are valuable compounds owing to their rich photochemical, electrochemical and catalytic properties that open the door to a wide range of applications in material science, photosynthetic processes, catalysis and energy
25 converting devices.¹ In particular, multiporphyrin arrays have attracted considerable attention due to their potential integration into energy converting devices owing to their crucial role in photosynthetic processes.² To reach a given spatial arrangement, numerous covalent spacers have been
30 tested such as phenyl, thiophene, ethynyl and aniline groups.³ Besides, direct connection of porphyrin units through oxidative C-C coupling shortens the distance leading to an higher electronic communication between these heterocycles. An important amount of studies reports the chemical synthesis
35 of directly linked porphyrin dimers, trimers and oligomers. Numerous chemical reagents such as Ag⁺,⁴ thallium(III)trifluoroacetate,⁵ tris(4-bromophenyl)aminium-hexachloroantimonate (BAHA),⁶ DDQ,⁷ hypervalent iodine (PhICl₂ and PhIF₂,⁸ PhI(OCOCF₃)₂ (PIFA)^{9,10} or PhI(OAc)₂,
40 (PIDA)⁹, mixtures of Ag⁺ and Au₃⁺ salts,¹¹ NaAuCl₄·2H₂O¹² and finally *m*-chloroperbenzoic acid¹³ have been successfully used for direct C-C coupling. This wide variety of oxidising agents proves that the choice of the right reactant is not
45 straightforward. At this point, oxidation of the monomer by electrochemical techniques seems an interesting green alternative, since it is possible to modulate the oxidative power of the working electrode thanks to the fine tuning of its

potential. The regioselectivity of the C-C coupling, *i.e.* *meso-meso*, *meso-β* or *β-β* depends principally on the metal inside
50 the porphyrin as well as its peripheral substitution pattern. In the case of magnesium(II) or zinc(II) porphyrins, only *meso-meso* coupling is observed, whatever the oxidant and/or the solvent. As very few examples of electrosynthesis of directly
55 linked dimers and/or oligomers exist,^{14,15,16} we recently reported optimized conditions for the selective and quantitative formation of the *meso-meso* dimer from electrochemical oxidation of the trisubstituted 5,15-ditolyl-10-phenylporphyrin zinc(II) (**1-Zn**).¹⁶ Contrary to zinc(II) porphyrins, few examples of oxidative coupling are reported
60 for nickel(II) porphyrins. This scarcity probably stems from the higher first oxidation potential of Ni(II) porphyrins which drastically limits the choice of efficient oxidizers. Furthermore, the regioselectivity of Ni(II) porphyrins coupling depends on the nature of the oxidant and/or the
65 solvent. For example, a *meso-β* coupling is reported with a Ni(II) 5,15-diarylporphyrin in a mixture of DDQ/Sc(OTf)₃ in toluene¹⁷ or by electrochemical oxidation in benzonitrile¹⁵ whereas *meso-meso* coupling occurs with Ni(II) 5,10,15-triarylporphyrins with PIFA in CH₂Cl₂.¹⁰ To the best of our
70 knowledge, only one electrochemical oxidative C-C coupling of nickel(II) porphyrins (5,15-diarylsubstituted) has been reported by Osuka and co-workers.¹⁵ This reaction produces regioselectively the *meso-β* dimer in 19.1% yield. Motivated by the finding of the principle(s) underlying this
75 regioselectivity, we turned our attention towards the redox reactivity of the triaryl-*meso*-substituted nickel(II) complex **1-**

Ni. Advantageously, this porphyrin exhibits only one free *meso* position and it can thus only lead to the dimer by oxidation. Additionally, as in the MOEP (M = Zn, H₂, Cu),^{18,19} MTPP (M = Zn, H₂)²⁰ and magnesium porphine series,²¹ **1-Ni** through oxidation must be prone to react with a wide range of nucleophiles offering the opportunity to functionalize the macrocycle. Also, the absence of substituent around the free *meso* position makes it possible to test the respective reactivities of the free *meso* and β positions. Moreover, it should be stressed that purification and characterization of an anodic nucleophilic substitution product has never been attempted with nickel porphyrins, probably because of an higher oxidation potential than zinc or magnesium complexes. Taking advantage of these unique features of **1-Ni**, our first results concerning its electrochemical oxidation in absence and in presence of nucleophiles (chloride and triphenylphosphine) are presented below.

Experimental

X-ray equipment and refinement. Diffraction data were collected on a Nonius KappaCCD diffractometer equipped with a nitrogen jet stream low-temperature system (Oxford Cryosystems). The X-ray source was graphite-monochromated Mo-K α radiation ($\lambda = 0.71073 \text{ \AA}$) from a sealed tube. Data were reduced by using DENZO software without applying absorption corrections; the missing absorption corrections were partially compensated by the data scaling procedure in the data reduction. The structure was solved by direct methods using the SIR92²² program and refined with full-matrix least-squares on F^2 using the SHELXL97²³ program with the aid of the WIN-GX²⁴ program suite. All non-hydrogen atoms were refined with anisotropic thermal parameters. Hydrogen atoms attached to carbon atoms were included in calculated positions and refined as riding atoms. For **3-Ni**, one of the chloroform molecule was found disordered over two positions with occupation factors converged to 0.60:0.40. One chloroform molecule was also found disordered with a pentane group with occupation factors respectively equal to 0.58:0.42.

Reagents and instrumentation

Tetraethylammonium hexafluorophosphate (TEAPF₆, Fluka puriss., electrochemical grade, $\geq 99.0\%$) and 2,6-lutidine (Aldrich, $\geq 99\%$) were used as received. Tetra-*n*-butylammonium hexafluorophosphate (TBAPF₆) was synthesized by mixing stoichiometric amounts of tetra-*n*-butylammonium hydroxide (Alfa-Aesar, 40% w/w aq. sol.) and hexafluorophosphoric acid (Alfa-Aesar, ca. 60% w/w aq. sol.). After filtration, the salt was recrystallized three times in ethanol and dried in oven at 80 °C for at least two days. CH₂Cl₂ (Carlo Erba 99.5%), CH₃CN (SDS, Carlo Erba, HPLC gradient 99.9%) and DMF (SDS, Carlo Erba, 99.9%) were distilled from P₂O₅, CaH₂ and CaH₂ respectively.

UV-visible absorption spectra were recorded with a Varian UV-vis spectrophotometer Cary 50 scan using quartz cells (Hellma). In spectroelectrochemical experiments, an UV-vis immersion probe (Hellma, $l = 2 \text{ mm}$) was connected through a fibre optic to the same spectrophotometer.

Mass spectra were obtained on a Bruker ProFLEX III spectrometer (MALDI-TOF) using dithranol as a matrix.

NMR spectra were measured on a BRUKER 300, 500 or 600 MHz spectrometer (Avance III Nanobay, Avance III, Avance II, respectively). The reference was the residual non-deuterated solvent.

Elemental analyses (C, H, N, S) were carried out on a Flash EA 1112 Thermo Electron analyzer.

All electrochemical manipulations were performed using Schlenk techniques in an atmosphere of dry oxygen-free argon at room temperature ($T = 20^\circ\text{C} \pm 3^\circ\text{C}$). The supporting electrolyte was degassed under vacuum before use and then dissolved at a concentration of 0.1 mol L⁻¹. Voltammetric analyses were carried out in a standard three-electrode cell, with an Autolab PGSTAT 302N potentiostat, connected to an interfaced computer that employed Electrochemistry Nova software. A double junction saturated calomel electrode (SCE) with background electrolyte between the two frits, was used as reference electrode. The auxiliary electrode was a platinum wire in an independent compartment filled with the background electrolyte and separated from the analysed solution by a sintered glass disk. For all voltammetric measurements, the working electrode was a platinum disk electrode ($\varnothing = 2 \text{ mm}$). In these conditions, when operating in a mixture of CH₂Cl₂/CH₃CN 4/1 (0.1 M TEAPF₆) the formal potential for the Fc⁺/Fc couple was found to be +0.40 V vs. SCE.

Bulk electrolyses were performed in a two or three-compartment cell separated by glass frits of medium porosity with an Amel 552 potentiostat coupled with an Amel 721 electronic integrator. A platinum wire spiral ($l = 53 \text{ cm}$, $\varnothing = 1 \text{ mm}$) was used as the working electrode, a platinum plate as the counter electrode and a saturated calomel electrode as the reference electrode. Electrolyses were followed by TLC and UV-visible absorption measurements. In the case of the three-compartment cell, a potential of 0.00 V/ECS was systematically applied after the oxidative electrolysis to extinguish the residual traces of cation radicals in solution.

Synthesis

5,15-ditolyl-10-phenylporphyrin nickel (II) **1-Ni**

160 mg of **1-H₂**¹⁶ (0.28 mmol) and 210 mg (0.84 mmol) of Ni(OAc)₂·2H₂O are dissolved in 20 mL of DMF. This mixture is degassed with argon during 10 min, and then heated at 160 °C during 30 min. After addition of 100 mL of CH₂Cl₂, the crude solution is washed three times with 200 mL of distilled water.

After evaporation of the solvent, purification on silica gel column chromatography (CH₂Cl₂) and recrystallisation from CH₂Cl₂/MeOH, **1-Ni** is obtained in 90% yield ($m = 158.4 \text{ mg}$).

¹H NMR (CD₂Cl₂, 300 MHz, 298 K): δ (ppm) 2.67 (s, CH₃, 6H), 7.53 (d, ³J = 7.8 Hz, *m*-Tol, 4H), 7.66-7.76 (m, *m*- and *p*-Ph, 3H), 7.93 (d, ³J = 7.8 Hz, *o*-Tol, 4H), 8.01-8.05 (m, *o*-Ph, 2H), 8.77 (d, ³J = 4.9 Hz, β -Pyrr, 2H), 8.82 (d, ³J = 4.9 Hz, β -Pyrr, 2H), 8.92 (d, ³J = 4.7 Hz, β -Pyrr, 2H), 9.17 (d, ³J = 4.7 Hz, β -Pyrr, 2H), 9.88 (s, *meso*, 1H); λ_{max} (CH₂Cl₂)/nm (log ϵ) 408 (4.97), 522 (3.86); MALDI-TOF MS (dithranol): [M]⁺ = 622.80.

Electrosynthesis

5-chloro-10,20-ditolyl-15-phenylporphyrin nickel (II) **1-Ni-Cl**

Electrolyses were carried out under argon, at room temperature,

in 32 mL of CH₂Cl₂/CH₃CN (4/1 v/v) containing 0.1 M of TEAPF₆, 20.0 mg (32.1 μmol) of **1-Ni** and 10 eq. of 2,6-lutidine (37 μl) in a two compartment cell under vigorous stirring ($\omega = 1350$ rpm). The applied potential was $E_{app} = 0.95$ V/SCE. At the end of the electrolysis, 15 F per mol of **1-Ni** were transferred. The solution mixture was then evaporated to dryness under reduced pressure. The resulting crude solid was dissolved in a minimum of CH₂Cl₂ and this solution was washed with 4×250 mL of distilled water to remove the supporting electrolyte. The organic phase was evaporated to dryness. The crude product was then purified by column chromatography on silica gel (CH₂Cl₂) and recrystallized from THF/H₂O to give **1-Ni-Cl** in 78% yield.

¹H NMR (CD₂Cl₂, 300 MHz, 298 K): δ (ppm) 2.65 (s, CH₃, 6H), 7.51 (d, ³J = 7.7 Hz, *m*-Tol, 4H), 7.64-7.74 (m, *m*- and *p*-Ph, 3H), 7.87 (d, ³J = 7.7 Hz, *o*-Tol, 4H), 7.96-8.00 (m, *o*-Ph, 2H), 8.69 (d, ³J = 5.0 Hz, β -Pyr, 2H), 8.72 (d, ³J = 5.0 Hz, β -Pyr, 2H), 8.82 (d, ³J = 5.0 Hz, β -Pyr, 2H), 9.49 (d, ³J = 5.0 Hz, β -Pyr, 2H); λ_{max} (CH₂Cl₂)/nm (log ϵ) 416 (5.42), 531 (4.27); MALDI-TOF MS (dithranol): [M]⁺ = 655.84. Elemental analysis: found: C, 72.57; H, 4.28; N, 8.00%. Calc. for C₄₀H₂₇ClN₄Ni·0.4H₂O: C, 72.24; H, 4.21; N, 8.42%.

5-triphenylphosphonium-10,20-ditolyl-15-phenylporphyrin nickel (II) **1-Ni-P**⁺

Electrolyses were carried out under argon, at room temperature, in 32 mL of CH₂Cl₂/CH₃CN (4/1 v/v) containing 0.1 M of TEAPF₆, 20.0 mg (32.1 μmol) of **1-Ni**, 10 eq. of 2,6-lutidine (37 μl) and 20 eq. of PPh₃ (171 mg). The applied potential was $E_{app} = 1.00$ V/SCE. At the end of the electrolysis, 2.0 F per mol of **1-Ni** were transferred. The solution mixture was then evaporated to dryness under reduced pressure. The resulting crude solid was dissolved in a minimum of CH₂Cl₂ and this solution was washed with 4×250 mL of distilled water to remove the supporting electrolyte. The organic phase was evaporated to dryness. The crude product was then purified on silica gel column chromatography (CH₂Cl₂), recrystallized from CH₂Cl₂/*n*-hexane providing **1-Ni-P**⁺ in 72% yield.

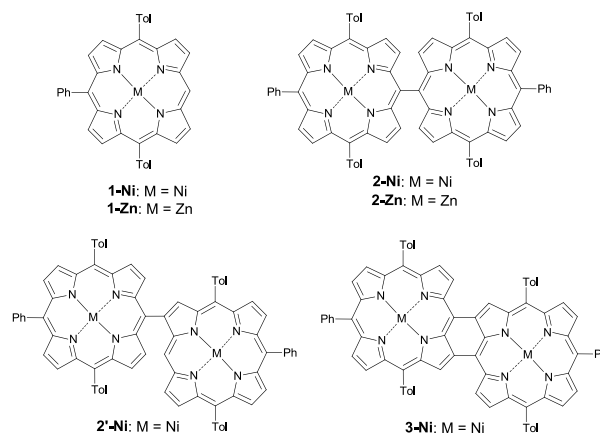
¹H NMR (CD₂Cl₂, 300 MHz, 298 K): δ (ppm) 2.58 (s, CH₃, 6H), 7.45 (d, ³J = 7.7 Hz, *m*-Tol, 4H), 7.71-7.86 (m, *m*- and *p*-Ph, *o*-Tol, 22H), 7.94-7.97 (m, *o*-Ph, 2H), 8.21 (d, ³J = 5.3 Hz, β -Pyr, 2H), 8.43 (d, ³J = 5.3 Hz, β -Pyr, 2H), 8.57 (d, ³J = 5.0 Hz, β -Pyr, 2H), 8.67 (d, ³J = 5.0 Hz, β -Pyr, 2H); ³¹P NMR (CD₂Cl₂, 121 MHz, 298 K): δ (ppm) 20.35 (s, phosphonium), -144.5 (hept, PF₆⁻); λ_{max} (CH₂Cl₂)/nm (log ϵ) 429 (5.18), 561 (3.78), 605 (3.96); MALDI-TOF MS (dithranol): [M-PF₆]⁺ = 882.88. Elemental analysis: found: C, 65.23; H, 4.29; N, 5.18%. Calc. for C₅₈H₄₂F₆N₄NiP₂·2H₂O: C, 65.37; H, 4.35; N, 5.26%.

Results and discussion

Voltammetric analysis of the oxidative reactivity of **1-Ni**

The novel Ni(II) 5,15-*p*-ditolyl-10-phenylporphyrin **1-Ni** (Scheme 1) was synthesized via metallation of the free-base **1-H₂**¹⁶ with nickel acetate in refluxing DMF. In agreement with C_{2h} symmetry, the ¹H NMR spectrum exhibits a singlet at 9.88 ppm corresponding to the *meso* proton and 4 doublets (β -pyrrolic protons) between 9.17 and 8.77 ppm.

All the potential values cited in this manuscript will be referred to the saturated calomel electrode (SCE). The cyclic voltammogram (CV) of **1-Ni** in CH₂Cl₂ containing 0.1 M



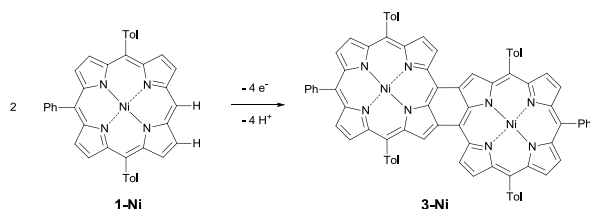
Scheme 1 Structures of the monomer (**1-Ni/1-Zn**), *meso-meso* dimer (**2-Ni/ 2-Zn**), *meso- β* dimer (**2'-Ni**) and *meso- β /meso- β* doubly-fused dimer (**3-Ni**).

TBAPF₆ (dotted line, Fig.1) exhibits two monoelectronic oxidations leading respectively to the cation- radical (peak system O1/R1, $E_p(O1) = 1.03$ V) and the dication (O2/R2, $E_{pa} = 1.25$ V).²⁵ This behaviour is roughly similar to the one observed for Ni(II)TPP (two monoelectronic and reversible oxidations proceeding on the macrocycle at $E_{1/2} = 1.01$ and 1.31 V/SCE).²⁶ Nevertheless, the behaviour of **1-Ni** is not so ideal: the first oxidation system is not chemically reversible, *i.e.* the intensity of R1 is drastically reduced compared to O1 ($i_{pa}/i_{pc} = 3.1$), which indicates the instability of the electrogenerated cation radical. Also, at the second stage, the peak is large and the current rise rather flat, which can originate in multiple species being oxidised at the same potential or a slowed electron transfer.

The CV of **1-Ni** undergoes drastic changes upon addition of 20% (vol.) acetonitrile in the initial CH₂Cl₂ solution (plain line, Fig. 1). Thus, the first oxidation process (peak O1', $E_p(O1') = 1.03$ V) becomes almost chemically irreversible, with an *ca.* 1.56 fold increase of the intensity. Unlike what is observed in pure dichloromethane solution, a second reversible peak system (O2'/R2') appears at $E_p(O2') = 1.25$ V as well as a new weak reduction peak, R4' ($E_p(R4') = 0.70$ V) on the backward scan.²⁷ Clearly, at the first oxidation stage, the addition of acetonitrile profoundly modifies the electrode reaction which product, at the scale of the voltammetric experiment, is no more longer the cation-radical **1-Ni**⁺, but a new compound oxidised at O2'. Following these observations, an important point was to identify this compound traced by the O2'/R2' peak system. Generally the chemical or electrochemical oxidation of Ni(II) porphyrins having at least one free *meso* position leads to the formation of *meso-meso* and/or *meso- β* singly-linked dimers which can be further oxidized to the *meso-meso*/ β - β /*meso-meso* triply-linked and *meso- β /meso- β* doubly-linked dimers, respectively. Except with PIFA as oxidant in CH₂Cl₂,^{9,10} the *meso- β* singly-linked and *meso- β /meso- β* doubly-linked dimers are the major products and their respective amount depends on the molar equivalent quantity of oxidants.²⁸ In an attempt to attribute the compound oxidized at peak O2', the singly bonded *meso-meso* dimer **2-Ni**⁹ and the *meso- β /meso- β* doubly-linked dimer **3-Ni**¹¹ were prepared independently and their respective CV (see Fig. 1) compared to the one of **1-Ni** in the CH₂Cl₂/CH₃CN mixture (80/20 v/v). If there is no apparent correspondence between the voltammograms

of **1-Ni** and **2-Ni**, the CV of **3-Ni** affords the same set of peaks O1'/R1', O2'/R2' and R4' as **1-Ni**.

The immediate conclusion is that the addition of acetonitrile catalyses the formation of the *meso-β/meso-β* doubly-linked dimer **3-Ni** at the first oxidation of **1-Ni**. The point is then to precise by which way or mechanism. First it should be stressed that the reaction is complex involving, for one dimer unit formed, 2 C-C couplings, 4 H⁺ releases and 4 electron uptakes (Scheme 2):



Scheme 2 Global reaction leading to doubly-fused **3-Ni** from **1-Ni**.

It seems unrealistic to propose a completely detailed mechanism. Nevertheless some hypotheses can be advanced concerning the catalytic influence of acetonitrile. Many studies concerning the electrochemistry of Ni(II) porphyrins have shown that parameters such as axial coordination, kind of solvent and/or the supporting electrolyte and temperature can switch the location of the electronic transfer from the ligand to the metal.²⁵

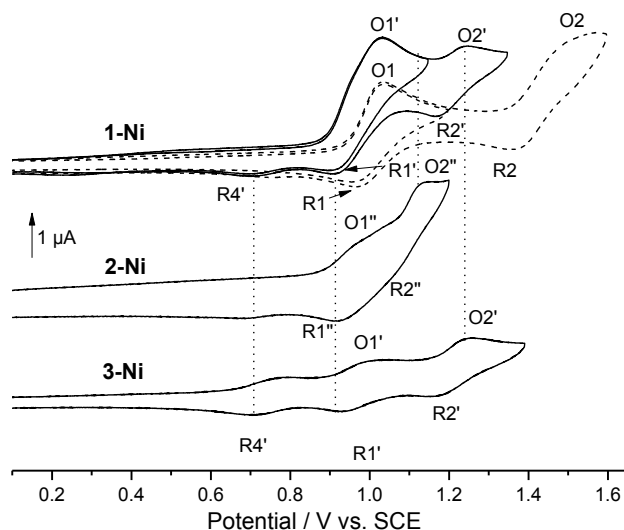


Fig. 1 Cyclic voltammograms of **1-Ni** (top), **2-Ni** (middle) and **3-Ni** (bottom) in CH₂Cl₂/CH₃CN (4/1 v/v) (solid line) and CH₂Cl₂ (dotted line) 0.1 M TEAPF₆. Concentration: 5×10⁻⁴ M for **1-Ni** and **2-Ni** and 3.8×10⁻⁴ M for **3-Ni**; WE: Pt Ø = 2 mm, ν = 100 mV s⁻¹).

For example, the Ni(II)TPP⁺ cation-radical electrogenerated by mono-electronic oxidation of Ni(II)TPP at room temperature in a non-coordinating solvent is converted into [Ni(III)TPP(L)₂]⁺ after addition of a coordinating solvent like THF, pyridine, benzonitrile or acetonitrile.²⁹ Thus, in our case, increase in the intensity of the first oxidation process upon addition of acetonitrile is ought to come from the simultaneous oxidation of Ni(II) and the porphyrin ligand into Ni(III) and the cation-radical, respectively.²⁷ The intermediate species would be thus the [**1-Ni(III)**]²⁺ dication probably incorporating one or two acetonitrile molecules as axial ligands. This intermediate is expected to be

highly reactive due to its electrodeficient character. For instance, it could immediately affect the C-C coupling by condensing a neutral unit of **1-Ni** hence accelerating the rate of the global reaction. At another level, the weakly basic property of acetonitrile³⁰ may facilitate the elimination of proton on the peripheral porphyrin positions engaged (or to be engaged) in the coupling and that may also result in a more rapid electrode reaction.

Encouraged by the apparent selective formation of **3-Ni** in cyclic voltammetry, the transposition at the electrolysis scale has been attempted.

Unexpected electro-synthesis of **1-Ni-Cl**

Electrolyses were carried out under argon, at room temperature, in a CH₂Cl₂/CH₃CN mixture (4/1 v/v) containing 0.1 M of TEAPF₆, **1-Ni** and 10 eq. of 2,6-lutidine, in a two compartment cell (anode and cathode in the same compartment). These conditions in the Zn series¹⁶ were demonstrated to afford one of the best selectivity in the formation of the *meso-meso* dimer, so, in a first attempt, they were retained for the oxidative electrolysis of **1-Ni**. The role of 2,6-lutidine is here to favor the elimination of protons accompanying the C-C coupling.

The applied potential ($E_{app} = 0.95$ V/SCE) corresponds to the first oxidation process of **1-Ni** in these conditions. Surprisingly, 15 F per mol of **1-Ni** were necessary for full conversion of the starting product whereas, in the Zn series, the needed amount of electricity was considerably lesser (2.5 F per mol).

The UV-vis. spectrum of the reacting solution of **1-Ni** has been monitored as a function of the electrolysis progress (Fig. 2), excluding the Soret band which could not be observed (massive absorption resulting in saturation of the measured signal).

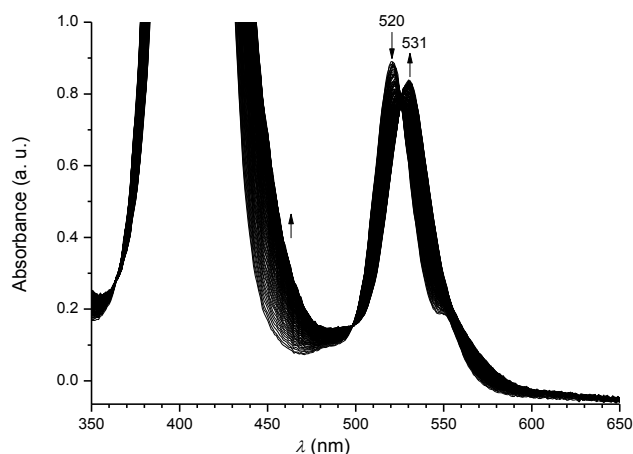


Fig. 2 Electrolysis of a 5×10⁻⁴ M solution of **1-Ni** with 10 equiv. of 2,6-lutidine followed by UV-vis spectroscopy ($l = 2$ mm, 0.1 M TEAPF₆ in CH₂Cl₂/CH₃CN (4/1 v/v), $E_{app} = 0.95$ V vs. SCE, -15 electrons, WE: Pt wire, WE and counter-electrode are in the same compartments).

The Soret band foot undergoes a progressive bathochromic shift while the initial Q band of **1-Ni** ($\lambda_{max} = 520$ nm) is progressively substituted by a new band at 531 nm. In addition, the presence of two isosbestic points at 498 and 526 nm confirms the simple transformation of the initial porphyrin into another well-defined product with no intermediate observed between. Contrary to our initial expectation, after extraction of the supporting electrolyte with water and purification of the crude solution, the *meso-*

Cite this: DOI: 10.1039/c0xx00000x

www.rsc.org/xxxxxx

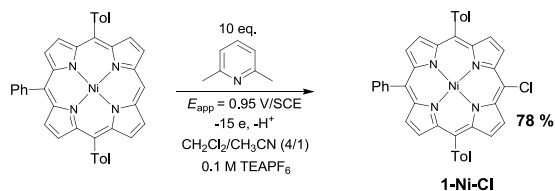
ARTICLE TYPE

Table 1 Product selectivity in the oxidative electrolysis of **1-Ni**.^a

Entry	Experimental conditions		Oxidation ^g		NMR yields ^d					
	Solvent	# of compartments	E_{app} (V/SCE)	Faraday vs. 1-Ni	1-Ni	1-Ni-Cl	2-Ni	2'-Ni	3-Ni	1-Ni-OH
1	DCM/ACN ^b	2	0.95	15.0	—	>95	—	—	—	—
2	DCM/ACN ^b	3	0.95	2.0	26	5	7	14	48	—
3	DCM ^c	3	0.95	2.0	7	24	14	55	—	—
4	CH ₃ CN ^e	—	—	—	—	—	—	—	—	—
5	THF ^f	2	1.20	—	—	—	—	—	—	—
6	DMF	3	1.10	5.5	<i>h</i>	<i>h</i>	<i>h</i>	<i>h</i>	<i>h</i>	<i>i</i>

^a Conditions common to all experiments: initial amount of **1-Ni** ($m = 6.3$ mg, $c = 5.0 \times 10^{-4}$ M), 10 molar equivalents of 2,6-lutidine vs. **1-Ni**, Pt anode and Pt cathode). ^b Experiments performed in dichloromethane (DCM)/acetonitrile (ACN) 4/1 v/v 0.1M TEAPF₆. ^c Experiments performed in DCM 0.1M TBAPF₆. ^d NMR yields calculated from the ¹H NMR spectrum of the crude electrolysed solution by integration of characteristic ¹H NMR signals of **1-Ni**, **1-Ni-Cl**, **2-Ni**, **2'-Ni** and **3-Ni** (see an example of calculation in ESI†). Precision of these measurements is estimated to be ca. ±2%. ^e **1-Ni** insoluble in CH₃CN. ^f Simultaneous oxidation of THF occurs at this potential. ^g In case of a three compartment cell configuration, the oxidation step is followed by a reduction step at $E_{app} = 0.00$ V/SCE. ^h Not detected by MALDI-TOF mass spectrometry. ⁱ Major product according to MALDI-TOF mass spectrometry, UV-vis. absorption spectroscopy and electrochemistry.

chlorinated porphyrin **1-Ni-Cl** was isolated in 78% yield (Scheme 3). Noteworthy, no **3-Ni** doubly-fused dimer was detected in the crude mixture. The molecular structure of **1-Ni-Cl** was confirmed by an independent synthesis proceeding by chemical chlorination of **1-Zn** with *N*-chlorosuccinimide (NCS),¹⁶ demetallation with TFA and then remetallation with nickel acetate. This procedure was chosen since direct chlorination of **1-Ni** with NCS was not successful.

**Scheme 3** Electrochemical synthesis of **1-Ni-Cl**.

Definite proof of the molecular structure was given from the X-ray diffraction analysis on single crystals of **1-Ni-Cl** (see below).

In an attempt to decipher the formation mechanism of the 5-chloro derivative **1-Ni-Cl**, different electrolysis conditions were tested. The crude electrolysed products were systematically analysed by MALDI-TOF MS and ¹H NMR, the latter method providing, in addition to the product's identity, their distribution (see all results in Table 1).§

When the electrolysis is carried out in the above-mentioned conditions but in a three compartment cell and with abstraction of only 2 F per mol, an intractable mixture of products is obtained from which **1-Ni**, **1-Ni-Cl**, **2-Ni**, **2'-Ni** and **3-Ni** are detected in a 26:5:7:14:48 NMR yield ratio, respectively (Table 1, entry 2). In the same conditions but without acetonitrile, **1-Ni**, **1-Ni-Cl**, **2-Ni**, **2'-Ni** are formed in a 7:24:14:55 NMR yield ratio respectively (Table 1, entry 3). Only traces of **3-Ni** are observed by UV-visible analysis thanks to its characteristic absorption band at 749 nm. By comparison of these two former experiments, it is interesting to note that the product distribution is quite different whether acetonitrile is present or not. In particular only traces of **3-Ni** are detected in CH₂Cl₂ whereas it is the major product in the

CH₂Cl₂/CH₃CN mixture. These results agree well with the CV analyses where the voltammetric signature of **3-Ni** is perfectly visible in the CH₂Cl₂/CH₃CN contrary to what is observed in CH₂Cl₂. Besides, in CH₂Cl₂, the *meso*-β-linked dimer **2'-Ni** is the major product (55%).

In order to avoid the parasite chlorination reaction sourced from CH₂Cl₂, electrolysis was attempted in pure CH₃CN but unfortunately, **1-Ni** was not soluble at all in this solvent (Table 1, entry 4).

THF was also tested (Table 1, entry 5) but it was impossible to perform an efficient electrolysis in this medium due to simultaneous oxidation of THF at the potential where **1-Ni** is oxidised.

In DMF, in a three compartment configuration (Table 1, entry 6), 5.5 F per mol were necessary for full conversion of **1-Ni**. At the end of the electrolysis, voltammetric analysis of the crude solution reveals one well-defined pseudo-reversible redox couple located at $E_{1/2} = 0.41$ V/SCE†. Besides, analysis of this solution by MALDI-TOF mass spectrometry shows one major peak at $m/z = 638$ corresponding to the hydroxyporphyrin **1-Ni-OH**.‡ Furthermore, the final UV-visible absorption spectrum ($\lambda_{max} = 416, 530$ and 570 nm) matches well with the one previously described for the very similar 5-hydroxy-10,15,20-triphenyl porphyrin Ni(II) described by Arnold and co-workers ($\lambda_{max} = 416.5, 529.5$ and 569 nm).‡³¹ Unfortunately, NMR characterization of this compound was impossible, even in presence of hydrazine or NaBH₄ as described previously, due to probable persistent traces of paramagnetic oxidized product. Formation of this compound reasonably results from an anodic nucleophilic substitution of **1-Ni** with OH⁻. Indeed hydroxide anion can be generated from residual water, in basic conditions (2,6-lutidine here). In summary, dichloromethane and the single compartment configuration are apparently necessary to produce **1-Ni-Cl** selectively. These results seem to indicate that CH₂Cl₂ is probably reduced at the cathode. According to Savéant and co-workers,³² the monoelectronic reduction of Ni(II) porphyrins in DMF, benzonitrile and 1,2-dichloroethane is centered on the

metal (Ni(II)→Ni(I)) rather than on the porphyrin ligand. Reactivity of this Ni(I) species was exploited for the electrocatalytic reduction of CH₃I,³³ which generates iodide ions and methyl radicals. The reduction of CH₃I is mediated by the Ni(I) intermediate which, via an inner-sphere mechanism, transfers its electron to iodomethane, regenerates the Ni(II) porphyrin and releases iodides in the solution. By analogy, reduction of **1-Ni(II)** into **1-Ni(I)** at the cathode may lead to the cleavage of CH₂Cl₂ leading to Cl⁻ and CH₂Cl[•] (Scheme 4). In the CH₂Cl₂/CH₃CN (4/1 v/v) mixture, the CV of **1-Ni** reveals a reduction peak R3' at $E_p(R3') = -1.37$ V (Fig. 3).

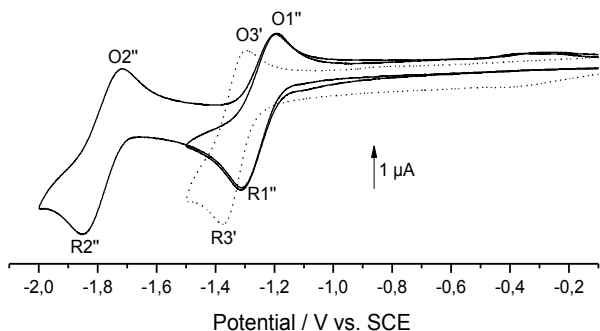
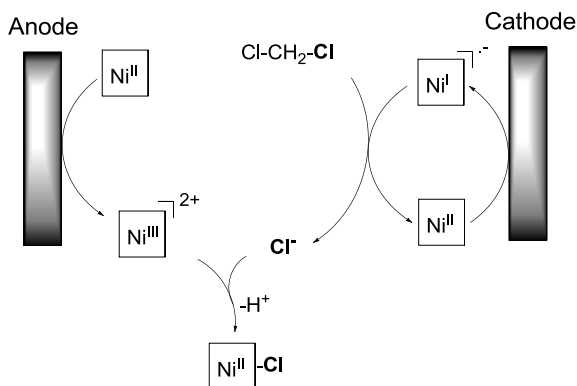


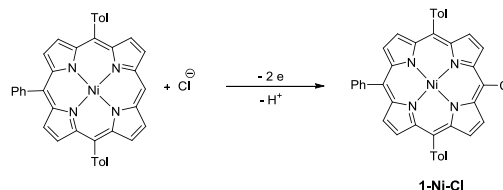
Fig. 3 Cyclic voltammograms of **1-Ni** (CH₂Cl₂/CH₃CN (4/1 v/v) (dotted line) and THF (solid line) containing 0.1 M TBAPF₆. Concentration: 5×10⁻⁴ M for **1-Ni** (WE: Pt ϕ = 2 mm, ν = 100 mV s⁻¹).

Supporting this assumption, the current ratio $i_p(R3')/i_p(O3'') = 0.39$ shows that this process is not reversible contrary to the one observed in THF which exhibits a current ratio $i_p(R1'')/i_p(O1'')$ closer to unity (0.78). Further, R3' is significantly higher than R1'' ($i_p(R3') = 1.16 \times i_p(R1'')$). These observations are in accordance with a slow catalytic process leading to CH₂Cl₂ decomposition. As a test for the real formation of chloride anions during the electroreduction of **1-Ni**, a controlled potential electrolysis ($E_{app} = -1.40$ V) in separated compartment in a mixture of CH₂Cl₂/CH₃CN (4/1 v/v) was performed. After an uptake of 1.0 F per mol, the electrolysed organic solution was extracted with distilled water. Ionic chromatography analysis of this aqueous phase confirms the presence of Cl⁻ in the amount of 0.93 molar equivalent of Cl⁻. This result confirms the effective formation of Cl⁻ by reduction of **1-Ni(II)** at its first reduction stage (faradaic yield: 93%).



Scheme 4 Proposed mechanism for the formation of **1-Ni-Cl**.

Since the release of Cl⁻ is now unambiguously established at the cathode, formation of **1-Ni-Cl** may stem from an anodic nucleophilic substitution of the free *meso*-position of **1-Ni** by Cl⁻ according to the global reaction in Scheme 5 and the mechanism proposed in Scheme 4:

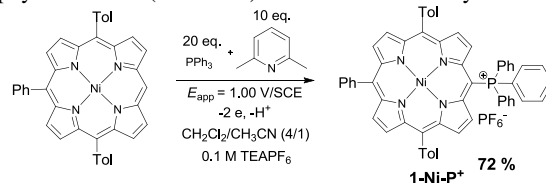


Scheme 5 Electrochemical synthesis of **1-Ni-Cl**.

Thus, the anodically electrogenerated [**1-Ni(III)**]²⁺, which intermediacy has been established by CV (see above) reacts with the cathodically produced Cl⁻. It should be stressed that the mechanism of anodic nucleophilic substitution proposed herein is thus an EECC type mechanism (C steps = addition of Cl⁻ and elimination of H⁺), contrary to what was previously reported for porphyrin complexes with electro-inactive metals such as zinc and magnesium (ECEC).¹⁸ Finally, to counterbalance the two electrons exchanged at the anode, the proton removed from the substituted position of the porphyrin should be reduced at the cathode. Nevertheless, this reaction leading to **1-Ni-Cl** lacks of efficiency. Indeed, total conversion of **1-Ni** is only accomplished after a transfer of 15 F per mol whereas the stoichiometry of the reaction let expect just two. To explain this result, several competing reactions can be envisioned: reverse reduction at the cathode of [**1-Ni(III)**]²⁺, comproportionation reaction of this latter with [**1-Ni(I)**]⁻ electrogenerated at the cathode and/or direct oxidation of chloride anions on the anode (chloride anions are oxidized near 1.00 V in our conditions), all possibly contributing to limiting the faradaic yield of the desired reaction.

Electrosynthesis of **1-Ni-P⁺**

As purification and characterization of compounds synthesized by anodic nucleophilic substitution of Ni(II) porphyrins have not been reported so far, we intended to test another nucleophile than chloride, *i.e.* triphenylphosphine (PPh₃). The electrolysis conditions were similar to those previously employed for the zinc derivative **1-Zn**: CH₂Cl₂/CH₃CN (4/1 v/v) containing 0.1 M TEAPF₆ as electrolyte, added of 20 eq. of PPh₃ and 10 eq. of 2,6-lutidine (*vs* **1-Ni**). Starting with 20 mg of **1-Ni** the potential was set at $E_{app} = 1.00$ V. 2.0 F per mol of **1-Ni** were transferred before the current dropped to zero. After removal of the supporting electrolyte, purification of the crude product on silica gel and crystallization from CH₂Cl₂/*n*-hexane, the *meso*-phosphonium porphyrin **1-Ni-P⁺** (Scheme 6) was isolated in 72% yield.



Scheme 6 Electrochemical synthesis of **1-Ni-P⁺**.

Fig. 4 is representative of the evolution of the UV-vis spectrum during the electrolysis. The Soret band undergoes a progressive bathochromic shift, in agreement with a functionalization of the

porphyrin core with an electro-withdrawing group (Fig. 4). The Q band, initially located at 521 nm, is gradually substituted by two new bands at 562 and 602 nm, which are associated to **1-Ni-P⁺**. No intermediate is observed between thus indicating a rather fast reaction after initiation by electron transfer.

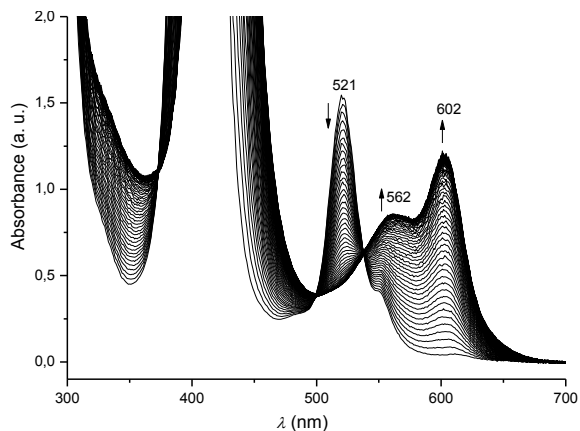


Fig. 4 Electrolysis of a 5×10^{-4} M solution of **1-Ni** with 10 equiv. of 2,6-lutidine and 20 equiv. of PPh_3 followed by UV-vis spectroscopy ($l = 2$ mm, 0.1 M TEAPF_6 in DCM/ACN 4/1 v/v, $E_{\text{app}} = 1.00$ V vs. SCE, -2.0 electrons, WE: Pt wire, WE and counter-electrode are in separated compartments).

Crystallography

As they were not reported yet, the crystallographic structures of **1-Ni**, **1-Ni-Cl**, **1-Ni-P⁺** and **3-Ni** were investigated in the course of this work. Suitable crystals for X-ray diffraction studies were obtained by slow diffusion of *n*-heptane into a CH_2Cl_2 solution of **1-Ni**, slow diffusion of *n*-hexane into a CH_2Cl_2 solution of **1-NiCl** or **1-NiP⁺** and slow diffusion of *n*-pentane into a CDCl_3 solution of **3-Ni**. Three-dimensional molecular views are presented on Fig. 5-8 and the most representative data are given in Table 2 (see also ESI for complete X-Ray data). As expected for Ni(II) porphyrins, **1-Ni** (Fig. 5), **1-Ni-Cl** (Fig. 6), **1-Ni-P⁺** (Fig. 7) and **3-Ni** (Fig. 8) deviate markedly from the planarity and no axial ligand is coordinated on the nickel(II) atom.³⁴ The usual square planar geometry of nickel(II) is confirmed here since it nearly lies in the mean plane formed by the 4 nitrogen atoms of the porphyrin: $0.0009 < d(\text{Ni-mean plane}_N) < 0.0640$ Å. **1-Ni**, **1-Ni-P⁺** and **3-Ni** exhibit a saddle shape conformation whereas the **1-Ni-Cl** porphyrin core adopts a ruffled conformation. The rms deviation from the planarity, *i.e.* the root mean square of the distances of the 24 carbon and nitrogen porphyrin ring atoms from the mean plane formed by these atoms were measured for these four complexes. According to these values, **1-Ni-P⁺** shows the strongest rms deviation (0.407 Å), followed by **3-Ni** (0.339 Å) then **1-Ni-Cl** (0.287 Å) and finally **1-Ni** (0.247 Å) expectedly following the order of steric encumbrance of the substitutive group at the differentiated *meso* position. Metal-nitrogen distances are longer for **1-Ni-Cl** and **1-Ni** than for **1-Ni-P⁺** and **3-Ni** ($1.936(5) < d < 1.942(5)$ Å, $1.941(3) < d < 1.955(3)$ Å, $1.906(5) < d < 1.918(5)$ Å, $1.906(2) < d < 1.926(3)$ Å, respectively, Table 2). In all cases, torsion angles between tolyl/phenyl groups and the porphyrin plane deviate markedly from orthogonality ($46.46(9)^\circ$ up to $83.33(5)^\circ$). Besides, $C_{\text{meso}}-C_{\text{ipso}}(\text{Tolyl/Phenyl})$ bonds are intermediate between a single and a double bond (between $1.479(8)$ and $1.508(9)$ Å).

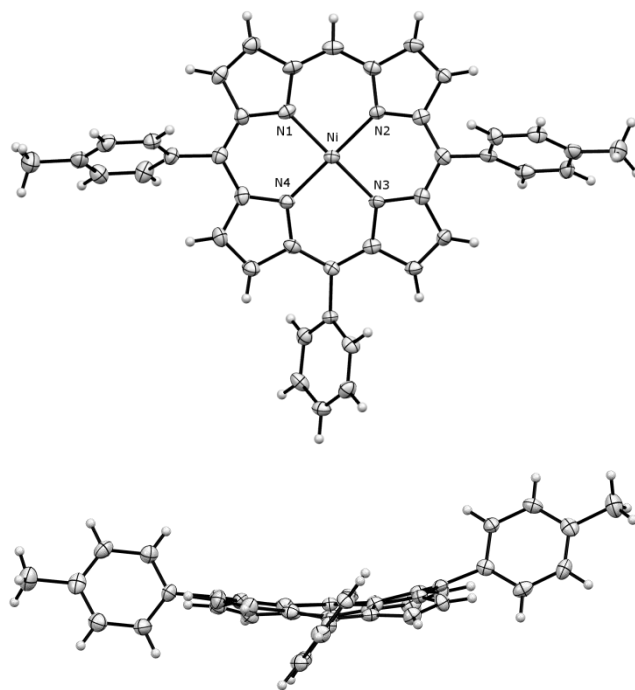


Fig. 5 Front and side Ortep views of **1-Ni** crystallographic structure (plot of **1-Ni** with 50% probability).

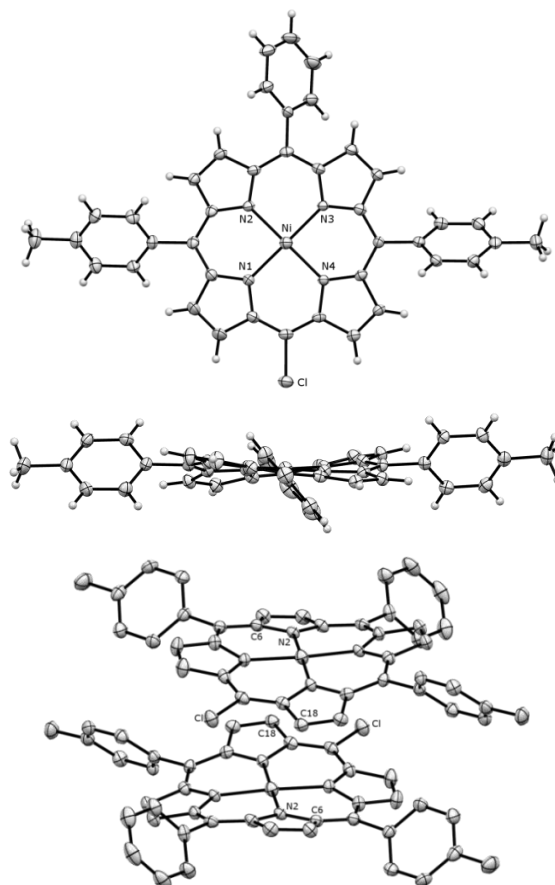


Fig. 6 Front (top) and side (middle) Ortep views of **1-Ni-Cl** crystallographic structure (*n*-hexane molecule omitted for clarity), Ortep view of the head to tail π -stacked dimer (bottom, H atoms omitted for clarity); plot of **1-Ni-Cl** with 50% probability.

Cite this: DOI: 10.1039/c0xx00000x

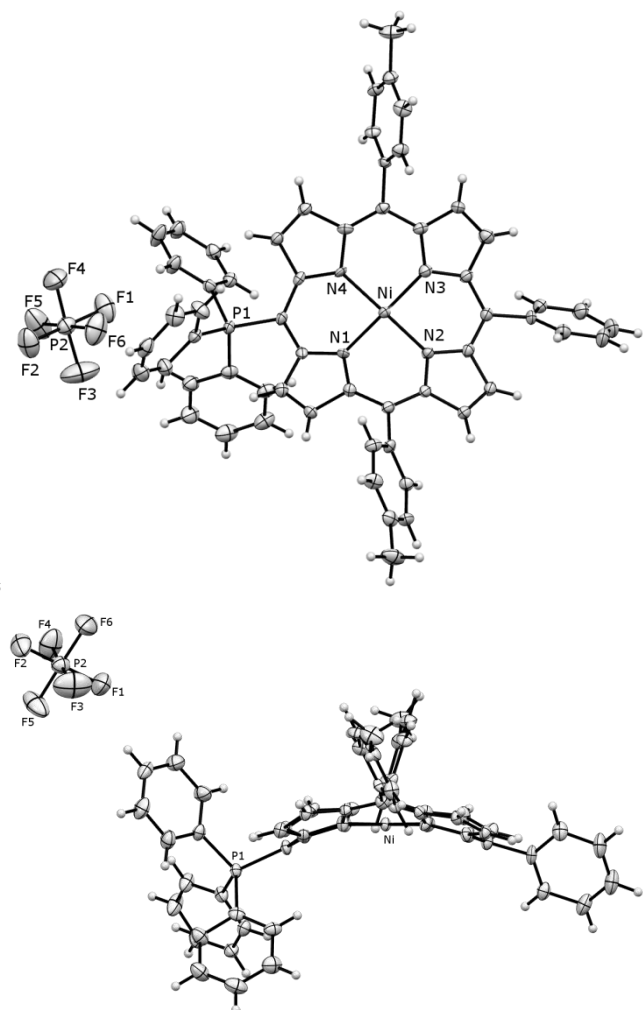
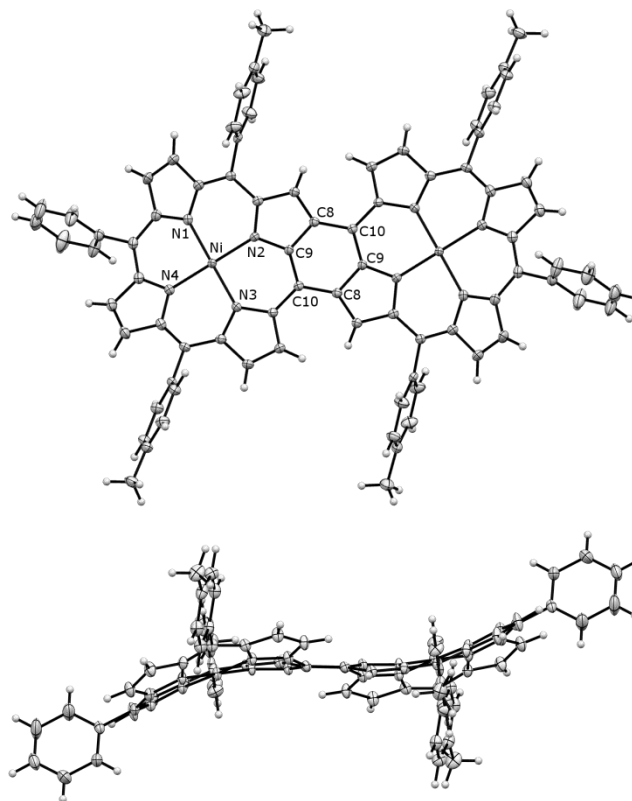
www.rsc.org/xxxxxxx

ARTICLE TYPE

Table 2 Selected structural parameters for **1-Ni**, **1-Ni-Cl**, **1-Ni-P⁺** and **3-Ni**.

	1-Ni	1-Ni-Cl	1-Ni-P⁺	3-Ni
$d(\text{Ni-mean plane}_N)^a$ (Å)	0.007(3)	0.002(1)	0.006(3)	0.011(1)
$d(\text{Ni-N})$ (Å)	1.936(5) < d < 1.942(5)	1.941(3) < d < 1.955(3)	1.906(5) < d < 1.918(5)	1.906(2) < d < 1.926(3)
Ph torsion angles ^b (°)	52.39(20)	49.34(9)	60.53(18)	70.43(9)
Tol torsion angles ^b (°)	66.69(17) / 69.03(18)	46.46(9) / 48.59(7)	62.26(16) / 73.69(16)	64.86(5) / 83.33(5)
$d(\text{C}_{\text{meso}}\text{-C}_{\text{Ph or Tol}})$ (Å)	1.479(8) < d < 1.500(8)	1.499(9) < d < 1.508(9)	1.492(5) < d < 1.502(5)	1.490(4) < d < 1.499(4)
RMS deviation ^c (Å)	0.247	0.287	0.407	0.339
$d(\text{C}_{\text{meso}}\text{-Cl})$ (Å)	d	1.746(4)	d	d
$d(\text{C}_{\text{meso}}\text{-P}^+)$ (Å)	d	d	1.809(6)	d
$d(\text{Ni}\cdots\text{Ni})$ (Å)	d	d	d	8.584(1)
$d(\text{meso-}\beta\text{ bond})$ (Å)	d	d	d	1.455(4)

^a Mean plane_N: mean plane calculated with the 4 nitrogen atoms of the porphyrin core. ^b Angle between the mean plane_p and the mean plane of the phenyl and tolyl groups. ^c The rms deviation corresponds to the root mean square of the distances of the 24 carbon and nitrogen porphyrin ring atoms from the mean plane formed by these atoms. ^d Not relevant.

**Fig. 7** Front and side Ortep views of **1-Ni-P⁺** crystallographic structure (H atoms omitted for clarity; plot of **1-Ni-P⁺** with 50% probability).**Fig. 8** Front and side Ortep views of **3-Ni** crystallographic structure (solvent molecules omitted for clarity, plot of **3-Ni** with 50% probability).

15 according to CCDC, 3 examples of free-base and zinc(II) *meso*-chloro porphyrins are reported (Fig. 6).³⁵ Interestingly, two molecules of **1-Ni-Cl** form an head to tail π -stacked dimer with a slipped cofacial orientation in a similar way to the photosynthetic special pair.³⁶ The interplanar and the centroid-to-centroid
20 (calculated from the 24 carbon and nitrogen porphyrin ring atoms) distances between parallel porphyrins are 3.554 and 4.627 Å, respectively. The difference in these two distances indicates that the porphyrin rings are significantly slipped. The slip angle

To our best knowledge **1-Ni-Cl** crystallographic structure is the
10 first representative of a *meso*-chloro Ni(II) porphyrin though,

(angle between the normal to the plane and the centroid-centroid vector) is 39.82° corresponding to a slippage distance of 2.96 Å. In particular, intermolecular interactions are observed between C6 and C18 ($d(C6\cdots C18) = 3.281(6)$ Å) and between N2 and C18 ($d(N2\cdots C18) = 3.207(5)$ Å) (Fig. 7). The $C_{meso}-Cl$ distance is 1.746(4) Å, an intermediate value as compared with the 3 other *meso*-chloro representatives (1.684-1.814 Å).

1-Ni-P⁺ is the second specimen of a *meso*-phosphonium porphyrin crystallographic structure reported so far (Fig. 7). The $C_{meso}-P^+$ distance is 1.809(6) Å, slightly longer than the one observed for the magnesium porphine derivative reported previously (1.794(4) Å).²¹

3-Ni represents, to our best knowledge, the third *meso-β/meso-β* doubly-fused dimer crystallographic structure reported so far (Fig. 8). In the three-dimensional structure both porphyrin core mean planes are perfectly coplanar though each porphyrin ring adopts a ruffled conformation. Both *meso-β* bonds are 1.455(4) Å long whereas the Ni⋯Ni distance is 8.584(1) Å. These values are very close to the ones reported previously by Osuka and co-workers⁶ for a similar nickel(II) *meso-β/meso-β* doubly-fused dimer (1.45 and 8.61 Å, respectively).

Conclusions

In summary the electrochemical oxidative reactivity of the tri-*meso*-substituted nickel(II) 5,15-*p*-ditolyl-10-phenylporphyrin complex **1-Ni** has been studied. An unexpected and efficient chlorination at the free *meso* position of **1-Ni** has been performed by oxidation in a CH₂Cl₂/CH₃CN mixture in a two compartment cell configuration. To mediate this reaction electrocatalytic reduction of CH₂Cl₂ occurs *via* the formation of [1-Ni(II)]⁻ at the cathode, which generates chloride anions in solution. These latter react with the anodically electrogenerated [1-Ni(III)]²⁺ finally producing the chlorinated derivative **1-Ni-Cl**. Besides, in a three compartment cell, addition of a coordinating solvent (CH₃CN) is necessary to produce the *meso-β/meso-β* doubly fused dimer **3-Ni** *via* the direct formation at the first di-electronic oxidation step of the [1-Ni(III)]²⁺ intermediate. CH₂Cl₂ is not the best solvent herein since it always leads to the formation of chlorinated side-products. Additionally, when used alone, it could not lead directly to **3-Ni** since the intermediate generated at the first mono-electronic oxidation step is not [1-Ni(III)]²⁺ but the cation radical [1-Ni(II)]⁺. In DMF, whatever the cell configuration, the hydroxyporphyrin **1-Ni-OH** is detected as the major product. Moreover, an efficient *meso*-functionalization of **1-Ni** has been performed by controlled potential electrolysis with triphenylphosphine as nucleophile leading to the phosphonium substituted derivative (**1-Ni-P⁺**).

This work echoes our recently reported results on the redox reactivity of the corresponding zinc(II) derivative **1-Zn** and its reaction towards the *meso-meso* dimer **2-Zn**.¹⁶ These studies have revealed that addition of the hindered base 2,6-lutidine as well as operating in DMF were the key parameters to obtain high yields of the desired *meso-meso* dimer. Anodic reactivity of **1-Ni** is here completely different since no dimer was obtained in DMF. Besides, 2,6-lutidine has no or very little effect on the voltammetric traces of **1-Ni** and during electrolysis experiment; the *meso-meso* dimer **2-Ni** is produced in very low yield contrary to the *meso-β* dimer **2'-Ni** or **3-Ni**, depending on the experimental

conditions.

This work is part of a more vast research program aiming at a better control of the oxidative reactivity of metalloporphyrins that is a prerequisite for the use of electrochemistry in the synthesis of designed porphyrin architectures. Herein, the central metal is demonstrated to be a decisive element in that sense. Further studies are in progress to improve the scope of the reaction.

Acknowledgements

The authors thank the Centre National de la Recherche Scientifique, the Conseil Régional de Bourgogne and the Université de Bourgogne for financial support. The authors are grateful to Sophie Fournier for technical support and to Dr. Benoît Habermeyer (PorphyChem Company) for a generous gift of **1-H₂**.

Notes and references

Institut de Chimie Moléculaire de l'Université de Bourgogne, Université de Bourgogne, CNRS UMR 6302, 9 avenue Alain Savary, 21078 Dijon Cedex, France. E-mail: charles.devillers@u-bourgogne.fr, dominique.lucas@u-bourgogne.fr; Fax: +33380396065; Tel: +33380399125.

§ On this occasion, in addition to **2-Ni** and **3-Ni**, the *meso-β* simply bonded dimer **2-Ni'** was synthesized independently; the reaction proceeds by oxidation of **1-Ni** with 2 eq. of DDQ and Sc(OTf)₃ in toluene at 50 °C.¹⁷ Thus, as for the other compounds, its specific signals could be distinguished in the ¹H NMR spectra of electrolyzed mixtures. Notably, as a unique feature, **2-Ni'** displays a singlet at 9.69 ppm in CDCl₃ and CD₂Cl₂, characteristic of its remaining *meso* proton.

† Electronic Supplementary Information (ESI) available: Characterisation data of **1-Ni**, **1-Ni-Cl**, **1-Ni-P⁺**, **2-Ni**, **2'-Ni** and **3-Ni**. See DOI: 10.1039/b000000x/

- F. J. Kampas, K. Yamashita and J. Fajer, *Nature*, 1980, **284**, 40;E. Song, C. Shi and F. C. Anson, *Langmuir*, 1998, **14**, 4315;C. Bucher, C. H. Devillers, J.-C. Moutet, G. Royal and E. Saint-Aman, *Chem. Commun.*, 2003, 888;H. Imahori, M. Kimura, K. Hosomizu, T. Sato, T. K. Ahn, S. K. Kim, D. Kim, Y. Nishimura, I. Yamazaki, Y. Araki, O. Ito and S. Fukuzumi, *Chem. Eur. J.*, 2004, **10**, 5111;L. Wei, K. Padmaja, W. J. Youngblood, A. B. Lysenko, J. S. Lindsey and D. F. Bocian, *J. Org. Chem.*, 2004, **69**, 1461;M. R. Wasielewski, *Acc. Chem. Res.*, 2009, **42**, 1910.
- I. Beletskaya, V. S. Tyurin, A. Y. Tsivadze, R. Guillard and C. Stern, *Chem. Rev.*, 2009, **109**, 1659.
- H. L. Anderson, *Chem. Commun.*, 1999, 2323;R. E. Martin and F. Diederich, *Angew. Chem. Int. Ed.*, 1999, **38**, 1350;C. O. Paul-Roth, J. Letessier, S. Juillard, G. Simonneaux, T. Roisnel and J. Rault-Berthelot, *J. Mol. Struct.*, 2008, **872**, 105;P. A. Liddell, M. Gervaldo, J. W. Bridgewater, A. E. Keirstead, S. Lin, T. A. Moore, A. L. Moore and D. Gust, *Chem. Mater.*, 2008, **20**, 135;J. Rault-Berthelot, C. Paul-Roth, C. Poriel, S. Juillard, S. Ballut, S. Drouet and G. Simonneaux, *J. Electroanal. Chem.*, 2008, **623**, 204.
- N. Yoshida, H. Shimidzu and A. Osuka, *Chem. Lett.*, 1998, **27**, 55.
- J. Wojaczyński, L. Latos-Grażyński, P. J. Chmielewski, P. V. Calcar and A. L. Balch, *Inorg. Chem.*, 1999, **38**, 3040.
- A. Tsuda, A. Nakano, H. Furuta, H. Yamochi and A. Osuka, *Angew. Chem. Int. Ed.*, 2000, **39**, 558;A. Tsuda, H. Furuta and A. Osuka, *J. Am. Chem. Soc.*, 2001, **123**, 10304.
- X. Shi and L. S. Liebeskind, *J. Org. Chem.*, 2000, **65**, 1665;M. O. Senge and X. Feng, *J. Chem. Soc., Perkin Trans. I*, 2000, 3615.

8. L.-M. Jin, J.-J. Yin, L. Chen, C.-C. Guo and Q.-Y. Chen, *Synlett*, 2005, **19**, 2893.
9. L.-M. Jin, L. Chen, J.-J. Yin, C.-C. Guo and Q.-Y. Chen, *Eur. J. Org. Chem.*, 2005, 3994.
10. Q. Ouyang, Y.-Z. Zhu, C.-H. Zhang, K.-Q. Yan, Y.-C. Li and J.-Y. Zheng, *Org. Lett.*, 2009, **11**, 5266.
11. A. K. Sahoo, Y. Nakamura, N. Aratani, K. S. Kim, S. B. Noh, H. Shinokubo, D. Kim and A. Osuka, *Org. Lett.*, 2006, **8**, 206.
12. D.-M. Shen, C. Liu, X.-G. Chen and Q.-Y. Chen, *J. Org. Chem.*, 2009, **74**, 206.
13. A. Takai, B. Habermeyer and S. Fukuzumi, *Chem. Commun.*, 2011, **47**, 6804.
14. T. Ogawa, Y. Nishimoto, N. Yoshida, N. Ono and A. Osuka, *Chem. Commun.*, 1998, 337; C. H. Devillers, D. Lucas, A. K. D. Dime, Y. Rousselin and Y. Mugnier, *Dalton Trans.*, 2010, **39**, 2404; M. A. Vorotyntsev, D. V. Konev, C. H. Devillers, I. Bezverkhyy and O. Heintz, *Electrochim. Acta*, 2010, **55**, 6703; M. A. Vorotyntsev, D. V. Konev, C. H. Devillers, I. Bezverkhyy and O. Heintz, *Electrochim. Acta*, 2011, **56**, 3436.
15. T. Ogawa, Y. Nishimoto, N. Yoshida, N. Ono and A. Osuka, *Angew. Chem. Int. Ed.*, 1999, **38**, 176.
16. A. K. D. Dime, C. H. Devillers, H. Cattey, B. Habermeyer and D. Lucas, *Dalton Trans.*, 2012, **41**, 929.
17. A. Tsuda, Y. Nakamura and A. Osuka, *Chem. Commun.*, 2003, 1096.
18. A. Giraudeau, L. Ruhlmann, L. El Kahef and M. Gross, *J. Am. Chem. Soc.*, 1996, **118**, 2969.
19. L. Ruhlmann, S. Lobstein, M. Gross and A. Giraudeau, *J. Org. Chem.*, 1999, **64**, 1352.
20. L. E. Kahef, M. E. Meray, M. Gross and A. Giraudeau, *Chem. Commun.*, 1986, 621; L. E. Kahef, M. Gross and A. Giraudeau, *Chem. Commun.*, 1989, 963; L. Ruhlmann and A. Giraudeau, *Chem. Commun.*, 1996, 2007; D. Schaming, Y. Xia, R. Thouvenot and L. Ruhlmann, *Chem. Eur. J.*, 2013, **19**, 1712.
21. C. H. Devillers, A. K. D. Dime, H. Cattey and D. Lucas, *Chem. Commun.*, 2011, **47**, 1893.
22. A. Altomare, G. Cascarano, C. Giacobozzo and A. Guagliardi, *J. Appl. Crystallogr.*, 1993, **26**, 343.
23. G. M. Sheldrick, Editon edn., University of Göttingen, Göttingen, Germany, 1997; G. Sheldrick, *Acta Cryst., Sect. A*, 2008, **64**, 112.
24. L. J. Farrugia, *J. Appl. Cryst.*, 2012, **45**, 849.
25. K. M. Kadish, E. V. Caemelbecke and G. Royal, in *The Porphyrin Handbook*, eds. K. M. Kadish, K. M. Smith and R. Guilard, Academic Press, 2000, vol. 8, pp. 1.
26. D. Chang, T. Malinski, A. Ulmann and K. M. Kadish, *Inorg. Chem.*, 1984, **23**, 817.
27. A. Wolberg and J. Manassen, *J. Am. Chem. Soc.*, 1970, **92**, 2982.
28. M. Kamo, A. Tsuda, Y. Nakamura, N. Aratani, K. Furukawa, T. Kato and A. Osuka, *Org. Lett.*, 2003, **5**, 2079.
29. J. Seth, V. Palaniappan and D. F. Bocian, *Inorg. Chem.*, 1995, **34**, 2201; D. Dolphin, T. Niem, R. H. Felton and I. Fujita, *J. Am. Chem. Soc.*, 1975, **97**, 5288.
30. K. Ikai, K. Takeuchi, T. Kinoshita, K. Haga, K. Komatsu and K. Okamoto, *J. Org. Chem.*, 1991, **56**, 1052.
31. L. J. Esdaile, M. O. Senge and D. P. Arnold, *Chem. Commun.*, 2006, 4192.
32. D. Lexa, M. Momenteau, J. Mispelter and J. M. Savéant, *Inorg. Chem.*, 1989, **28**, 30.
33. K. M. Kadish, M. M. Franzen, B. C. Han, C. Araullo-McAdams and D. Sazou, *J. Am. Chem. Soc.*, 1991, **113**, 512; K. M. Kadish, M. M. Franzen, B. C. Han, C. Araullo-McAdams and D. Sazou, *Inorg. Chem.*, 1992, **31**, 4399.
34. K.-i. Yamashita, K. Kataoka, M. S. Asano and K.-i. Sugiura, *Org. Lett.*, 2012, **14**, 190.
35. S. Ito, L. T. Phong, T. Komatsu, N. Igarashi, S. Otsubo, Y. Sakai, A. Ohno, S. Aramaki, Y. Tanaka, H. Uno, T. Oba and K. Hiratani, *Eur. J. Org. Chem.*, 2009, **2009**, 5373.
36. J. Deisenhofer and H. Michel, *Science*, 1989, **245**, 1463.